The role of *Grg4* in tectal laminar formation

Sayaka Sugiyama* and Harukazu Nakamura†

Department of Molecular Neurobiology, Institute of Development, Aging and Cancer, and Graduate School of Life Sciences, Tohoku University, Seiryo-machi 4-1, Aoba-ku, Sendai 980-8575, Japan
*Present address: Laboratory for Neuronal Circuit Development, Brain Science Institute, RIKEN, 351-0198 Japan
†Author for correspondence (e-mail: nakamura@idac.tohoku.ac.jp)

SUMMARY

Mature chick optic tecta consist of 16 laminae and receive retinal fiber projections in a precise retinotopic manner. Retinal axons arborize in laminae a-f of the SGFS, but do not cross the border between lamina f and g. In order to elucidate molecular mechanisms of tectal laminar formation, we first looked at the migration of tectal postmitotic cells. We found that the migration pattern of postmitotic cells changes around E5 and that late migratory cells intervened laminae that were formed by early migratory cells. The coincident appearance of *Grg4* expression in the tectal ventricular layer and the change in migration pattern suggested an important role for *Grg4*.

Clonal misexpression of *Grg4* resulted in cells migrating to laminae h-j of the SGFS. Massive misexpression of *Grg4* resulted in disruption of laminae that were formed by early migratory cells, in particular lamina g of the SGFS. Application of *Grg4* morpholino antisense oligonucleotide or the misexpression of a dominant-negative form of *Grg4* exerted the opposite effect. We concluded that *Grg4* may direct tectal postmitotic cells to follow a late migratory pathway.

Key words: *groucho*, *En*, Cell fate, Lamination, Retinotectal projection, Remodeling

INTRODUCTION

Most neurons that make up the vertebrate nervous system arise from the ventricular layer. After proliferating in the ventricular layer, postmitotic neuronal cells migrate to their ultimate destination. The fate of postmitotic neuronal cells is dependent on the place and time of their birth (reviewed by Jacobson, 1991). Migration of these cells has been extensively analyzed in the cerebral cortex, where 'inside-out' type migration takes place (McConnell, 1988; Jackson et al., 1989). In reeler mice, where inside-out migration is disrupted, neurons that have been unable to reach their correct position still possess their morphological property (reviewed by Pearlman et al., 1998; Rice and Curran, 1999; Hevner et al., 2001). Thus, the question is raised as to how these cells become programmed within the ventricular layer.

Although the chick optic tectum also displays laminar structure (LaVail and Cowan, 1971a), the manner of postmitotic neuronal cell migration varies slightly from that in the cerebral cortex (LaVail and Cowan, 1971b; Gray et al., 1988; Gray and Sanes, 1991). LaVail and Cowan (LaVail and Cowan, 1971b) reported that the tectal laminae were formed as a result of three distinct migration waves; the first wave forms the inner lamina, the second one forms the outer lamina and the last one forms the middle lamina (LaVail and Cowan, 1971b). In the central part of the tectum, the first and the second waves overlap chronologically; the first was between E3 and E5 and the second was between E4 and E7. The third wave occurred between E6 and E8.

Grg4 belongs to the *Gro/Grg/TLE* family and functions as a transcriptional repressor by binding to specific transcriptional factors (Cavallo et al., 1998; Roose et al., 1998) (reviewed by Fisher and Caudy, 1998; Chen and Courey, 2000; Courey and Jia, 2001). In our previous paper we showed that *Grg4* is expressed in the prosencephalon and the mesencephalon at E2, and suggested that *Grg4* antagonizes isthmus organizing activity to set the anterior limit of the tectum (Sugiyama et al., 2000). Further study has revealed that *Grg4* expression ceases during E3 and E4, reappearing at E5. After E5, *Grg4* expression is seen in the ventricular layer. In the spinal cord, *Grg* is implicated in determining the fate of neuronal progenitor cells along the ventrodorsal axis (Muhr et al., 2001). As migration patterns change around E5 (LaVail and Cowan, 1971b), we proposed that *Grg4* might be involved in changing the fate of tectal postmitotic cells. To test this hypothesis, we first examined the migration pattern of tectal postmitotic cells by pulse-labeling the tectal neuroepithelium with *lacZ*. Our results demonstrated that the migration pattern changed around E5, coinciding with the re-expression of *Grg4*. Next, we used a retroviral vector and the morpholino antisense oligonucleotide to perform gain- and loss-of-function experiments. We concluded that *Grg4* imbibes ventricular cells with a late migratory fate. In addition, lamina g, which is normally unreceptive to the invasion of retinal axons (Yamagata and Sanes, 1995), was disrupted by the misexpression of *Grg4*, allowing retinal axons to invade the deeper laminae.

MATERIALS AND METHODS

Chick embryos

Virus-sensitive and conventionally raised fertile chick eggs were

purchased from Nisseiken and from a local farm, respectively. They were incubated at 38ºC in a humidified atmosphere and were staged according to Hamburger and Hamilton (Hamburger and Hamilton, 1951).

Introduction of plasmids and morpholino antisense oligonucleotide

Pulse-labeling of the neuronal progenitor cells of the optic tectum was achieved by transfecting at E3, E5 or E6 with the *lacZ* expression vector, pMiwZ (Suemori et al., 1990) using in ovo electroporation (Funahashi et al., 1999; Momose et al., 1999; Nakamura et al., 2000; Summerton, 1999).

Misexpression of *Grg1* and *Grg4* was achieved by electroporation on E2 embryos (at stage 9-11) with retroviral plasmid vector. Expression of the gene of interest may spread from the originally transfected cells in virus-sensitive embryos by infection with the virus. In virus-insensitive embryos, misexpression is limited to the descendents of the originally transfected cells. The entire coding regions of *Grg1* and *Grg4*, as well as the 5′-region of *Grg4* (*Grg4-5′*) with an HA-tag sequence (Sugiyama et al., 2000), were inserted into Cla12 adapter plasmids. Each *Cla*I fragment of cDNA (~2.4 kb) was then subcloned into the retroviral vector RCAS(BP)B (Hughes et al., 1987). The RCAS(BP)B-AP vector, into which alkaline phosphatase (AP) had been subcloned, served as a control (Cepko et al., 2000). To increase the survival rate of embryos, we used the tungsten microelectrode as the cathode and the platinum electrode as the anode. A square pulse of 7-8 V for 25 mseconds was delivered and the electroporator was charged twice (Momose et al., 1999).

Retrovirus infection was also performed. The retroviral fluid for RCAS(BP)B-En2, into which chick *En2* had been subcloned (Shigetani et al., 1997), was injected into the lumen of the mesencephalon in virus-sensitive embryos at E2 (stage 8-9).

The sequence of fluorescein-labeled morpholino antisense oligonucleotide for *Grg4* (Gene Tools) was 5′-GCGGATCATC-CACGCCGCTTCGGG-3′. The supplier's recommended control oligonucleotide, 5′-CCTCTTACCTCAGTTACAATTTATA-3′, was used. A 1 mM solution of control or *Grg4* morpholino was injected into the aqueductus mesencephali at stage 28, and electroporation was carried out as described above. As fluorescein-labeled morpholino is positively charged, it was introduced on the cathode side.

In situ hybridization, immunohistochemistry and histochemistry

In situ hybridization on sections was performed as described by Ishii (Ishii et al., 1997). Hybridization was carried out at 65ºC. Digoxigenin (DIG)-labeled RNA probes of *Grg1* (corresponding to amino acids 2-255), *Grg4* (Sugiyama et al., 2000), *ER81* (kind gift from Dr Matsunaga), *Lim1* (Matsunaga et al., 2000), *Sox2*, *Sox14* (Uchikawa et al., 1999) and *Cash1* (Jasoni et al., 1994) were used.

The following primary antibodies were used for immunohistochemistry; anti-β-galactosidase (rabbit polyclonal, ICN), anti-Hu-C/D, 16A11 (monoclonal, Molecular probes), anti-HA, 3F10 (monoclonal, Roche), anti-HA (rabbit polyclonal, Upstate), anti-neurofilament, 3A10 (monoclonal, Developmental Studies Hybridoma Bank (DSHB)), anti-Parvalbumin, PARV-19 (monoclonal, Sigma), anti-Glutamate (rabbit polyclonal, Sigma), anti-NgCAM, 8D9 (monoclonal, DSHB), anti-En, 4D9 (monoclonal, DSHB) and anti-gag, AMV-3C2 (monoclonal, DSHB). Cy3- or Alexa 488-conjugated goat anti-mouse, anti-rabbit or anti-rat antibodies were used as secondary antibodies (Jackson, Molecular Probes, Rockland).

Sections of RCAS(BP)B-AP-infected embryos were processed for AP activity (Halliday and Cepko, 1992), or were immunostained with anti-gag antibody. For the AP reaction, endogenous AP was inactivated by heating to 65ºC for 30 minutes. Sections were then placed in AP buffer containing 0.1 mg/ml X-phosphate (5-Bromo-4Chloro-3-indolyl-phosphate, Roche), 1 mg/ml Nitro Blue Tetrazolium (Roche) and 1 mM levamisole (Sigma), until the color was developed.

For nuclear staining, sections were incubated in 1-10 µg/ml DAPI (4′ 6-Diamidino-2-phenylindole Dihydrochloride) in PBT and mounted in 2.3% DABCO (Sigma) in 80% glycerol.

BrdU incorporation

BrdU (Bromodeoxyuridine) solution (10 mM, Sigma) was injected into the aqueductus of the retrovirus-infected mesencephalon at E8. Two hours after BrdU injection, the embryos were fixed in 4% paraformaldehyde in PBS. Incorporated BrdU was detected by the addition of monoclonal anti-BrdU antibody (Roche), followed by incubation with Cy3-conjugated anti-mouse secondary antibody.

Labeling of retinal axons

Retinal ganglion cells were labeled with 25% horseradish peroxidase (HRP, Toyobo) in Hanks' buffer or with a tiny crystal of a tiny crystal of DiI (1,1′-dioctadecyl-3,3,3′,3′-tetramethylindocarbocyanine perchlorate, Molecular Probes) at E15. The embryos were fixed in 4% paraformaldehyde at E17. To reveal the retinal fibers targeting the deep tectal lamina, the tecta after DiI labeling were cut into 100 µm sections on the vibratome (Dosaka EM) and observed under a fluorescence microscope, or the tecta after HRP labeling were cut into 100 µm section and were stained immunohistochemically using a primary rabbit anti-HRP antibody (polyclonal, Biogenesis) and a secondary Cy3-conjugated anti-rabbit antibody. The sections were then immunostained with anti-gag antibody and *Grg4* misexpression was assessed.

RESULTS

Early and late migratory waves from the neuroepithelium

The mature chick optic tectum consists of 16 laminae: SO (stratum opticum), SGFS (stratum griseum et fibrosum superficiale, a-j), SGC (stratum griseum centrale), SAC (stratum album centrale), SGP (stratum griseum periventriculare), SFP (stratum fibrosum periventriculare) and ependyma. The time of origin and the pattern of cell migration in each lamina have been previously studied by cumulative labeling of [3H] thymidine (LaVail and Cowan, 1971b) (Fig. 1A). Tectal laminae are formed as a result of three migration waves: the first one is between E3 and E5, and is to the deeper strata (SGC, SAC, SGP and SFP); the second one is between E4 and E7, and reaches the outer laminae (laminae a-g) of the SGFS; and the third one is between E6 and E8, to the inner laminae (laminae h-j) of SGFS.

In the tectum at E8, most cells are postmitotic (LaVail and Cowan, 1971b) and five laminae are formed (Fig. 1A): two thin laminae (IV, III), a cell-filled thick lamina (II), a fiber-rich lamina (I) and the ventricular layer. These laminae are reorganized into 13 laminae by E12, by mechanisms that are not yet fully understood. As it is difficult to pulse-label progenitor cells with [3H]-thymidine or BrdU in the chick tectum, we took advantage of in ovo electroporation techniques and transfected a *lacZ* expression vector, pMiwZ. Expression from pMiwZ is transient, peak expression being around 24 hours after electroporation (Funahashi et al., 1999; Momose et al., 1999). In rapidly proliferating cells, plasmid and translation products are diluted rapidly (Funahashi et al., 1999). In stable cells, high levels of the introduced gene product are still maintained at 2 weeks after electroporation (Aihara and Miyazaki, 1998; Kishimoto et al., 2002). We carried out electroporation with pMiwZ at E5 to check if this method could be used to pulse-label neuroepithelial cells. By E5, many
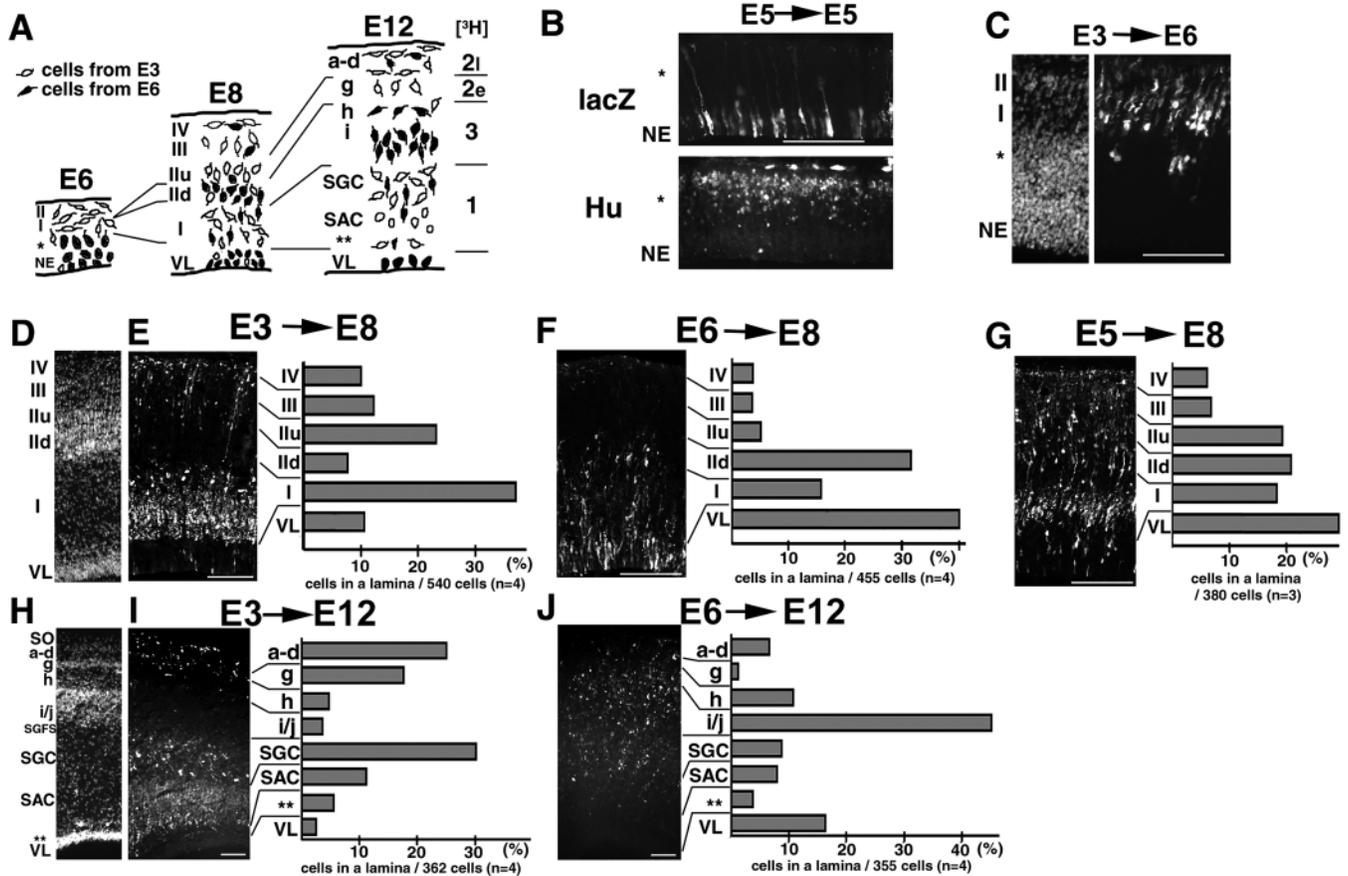
Fig. 1. Laminar formation of the tectum. (A) Laminar formation by early and late migratory cells. (B) Two hours after electroporation with *lacZ* vector at E5. (Upper panel) Immunohistochemistry with anti-*lacZ*. (Lower panel) Immunohistochemistry with anti-Hu-C/D. Hu-positive early neurons accumulate in the upper layer of the ventricular layer before migrating into their destination, so this layer could be distinguished as the early neuronal layer (∗). *lacZ* staining is observed in the neuroepithelial layer, not in the early neuronal layer at 2 hours after electroporation. NE, neuroepithelial layer. (C) Horizontal section of an E6 tectum that was labeled at E3. DAPI staining (left panel) reveals laminae I and II and the ventricular layer. In the ventricular layer, the early neuronal layer could be distinguished (∗). Cells labeled at E3 migrate out of the neuroepithelium and make up lamina II and I by E6. (D,H) DAPI staining of E8 (D) and E12 (H) tecta to show laminar formation. (E-G) Distribution of *lacZ*-positive cells at E8. Electroporation with pMiwZ was carried out at E3 (E), E6 (F) and E5 (G). Left panel shows *lacZ* staining, and right panel shows the number of *lacZ*-positive cells in each lamina. (I,J) Distribution of *lacZ*-positive cells at E12. Electroporation with pMiwZ was carried out at E3 (I) and E6 (J). Left panel shows *lacZ* staining, and right panel shows the number of *lacZ*-positive cells in each lamina. As the cells labeled at E6 migrated into lamina IId (F), these cells (late migratory cells) may have divided the laminae that had been formed by early migratory cells (C). Thus, the laminae of early migratory cells are split into two (E): upper laminae (laminae IV-IIu) and deeper lamina (lamina I). Distribution of late migratory cells at E8 and E12 indicates that lamina IId at E8 is remodeled to laminae h and i/j of the SGFS (F,J). E5 is the transitory stage and the ventricular layer may be composed of a mixture of the progenitors of early and late migratory cells. Thus, the cells labeled at E5 showed ubiquitous distribution (G). Scale bars: 100 μm.

cells in the tectum are postmitotic (LaVail and Cowan, 1971b), but postmitotic cells pile up in the ventricular layer until about E5 (stage 27) (Gray and Sanes, 1991). Cells that express Hu-C/D, a marker for the early neuron, accumulate just over the neuroepithelium as shown in the spinal cord (Wakamatsu and Weston, 1997). We designated this layer as early neuronal (Fig. 1A,B). Two hours after electroporation at E5, the *lacZ*-positive cells were restricted to the neuroepithelium and were not seen in the Hu-C/D-positive early neuronal layer (Fig. 1B), indicating that in ovo electroporation with pMiwZ could be used for pulse-labeling of neuroepithelial cells.

First, we carried out electroporation at E3 (stage 16-18). At E6 (stage 29), labeled cells were found in laminae II and I (Fig. 1C). In lamina I, the labeled cells extended their fibers to

migrate to their destination. At E8, the cells that had been labeled at E3 were found in lamina I (37%), upper lamina II (24%), lamina III (12%) and lamina IV (10%). Deeper within lamina II, labeled cells were hardly found (7%, Fig. 1D,E), suggesting that lamina II should be divided into two subregions: upper lamina II and deeper lamina II.

The cells labeled at E6 (stage 29-30) were found in the deeper lamina II (32%) and lamina I (16%) by E8 (Fig. 1F), but were hardly found (4-5%) in the upper laminae (i.e. laminae IV-IIu). Many labeled cells stayed in the ventricular layer (40%). The fact that cells labeled at E6 had colonized into the deeper region of lamina II, but not into the upper region, supports the proposition that lamina II is composed of two sublaminae.

As the migration behavior was different between the cells that were labeled around E3 and those that were labeled around E6, we focused on the behavior of cells that were labeled in between. We carried out electroporation at E5 with pMiwZ and looked at localization of labeled cells at E8. As expected, labeled cells studded entire laminae (Fig. 1G). The results indicate that the migration pattern of postmitotic cells in the tectum changes around E5. We designated those that migrate before E5 as early migratory cells, while those that migrate after E5 were referred to as late migratory cells. At E5, the tectal neuroepithelium may be in a transitory state and be composed of a mixture of early and late migratory cells.

At E12, we could distinguish 13 laminae: SO, SGFS (a/b, c, d, g, h, i, j), SGC, SAC, SGP, SFP and the ventricular layer. Most cells that were labeled at E3 were found in two distinct zones: some were in the deeper laminae such as the SGC (30%) and SAC (11%), while others were in the upper laminae such as laminae a-d (25%) and g (17%) of the SGFS (Fig. 1H,I). Comparison of the pattern of distribution of the labeled cells at E8 and E12 after electroporation at E3 indicates that lamina I at E8 may be reorganized into deeper laminae (SGC and SAC), and that laminae IV-IIu at E8 may be reorganized into the upper laminae (a-d and g of SGFS) at E12.

The majority of cells labeled at E6 were found in laminae i/j (45%), and h (11%) of the SGFS at E12 (Fig. 1J). This result, together with that seen at E8 indicates that lamina IId at E8 is reorganized into laminae i/j and h of the SGFS at E12. Labeled cells were also found in the SGC (9%) and SAC (8%). These cells may be those that are still migrating toward the destination, as they extend radial processes. Thus, the SAC and SGC may be composed of early migratory cells.

Expression of *Grg4* and *Grg1* during tectal lamination

Previously, we have reported that *Grg4* is expressed in the mesencephalon and prosencephalon at E2, where it plays an important role in the boundary formation and rostrocaudal polarity formation of the tectum by repressing En2 (Sugiyama et al., 2000; Ye et al., 2001). The expression of *Grg4* ceases during E3-E4 and then reappears at E5. We examined the precise expression pattern of *Grg4* to determine whether it plays a role in regulating the migration pattern of postmitotic cells.

At E4 (stage 22), *Grg4* expression transiently disappeared from the tectal anlage (Fig. 2B). *Grg4* was re-expressed at late E5 (stage 28) in the ventricular layer in a gradient rostrocaudally: rostral high and caudal low (Fig. 2C,D). Because of this gradient, the level of *Grg4* expression at the rostral part of the tectum at late E5 is similar to that at the caudal part at E6 (stage 29, Fig. 2D,E). Although *Grg4* expression was seen throughout the ventricular layer, cells that strongly expressed

Grg4 gathered at the outermost zone, as the early neuronal layer. Double-staining for *Grg4*, using in situ hybridization, and for Hu-C/D, using immunohistochemistry, shows that cells that are strongly positive for *Grg4* also express Hu-C/D (Fig. 2E). This result indicates that these cells are postmitotic
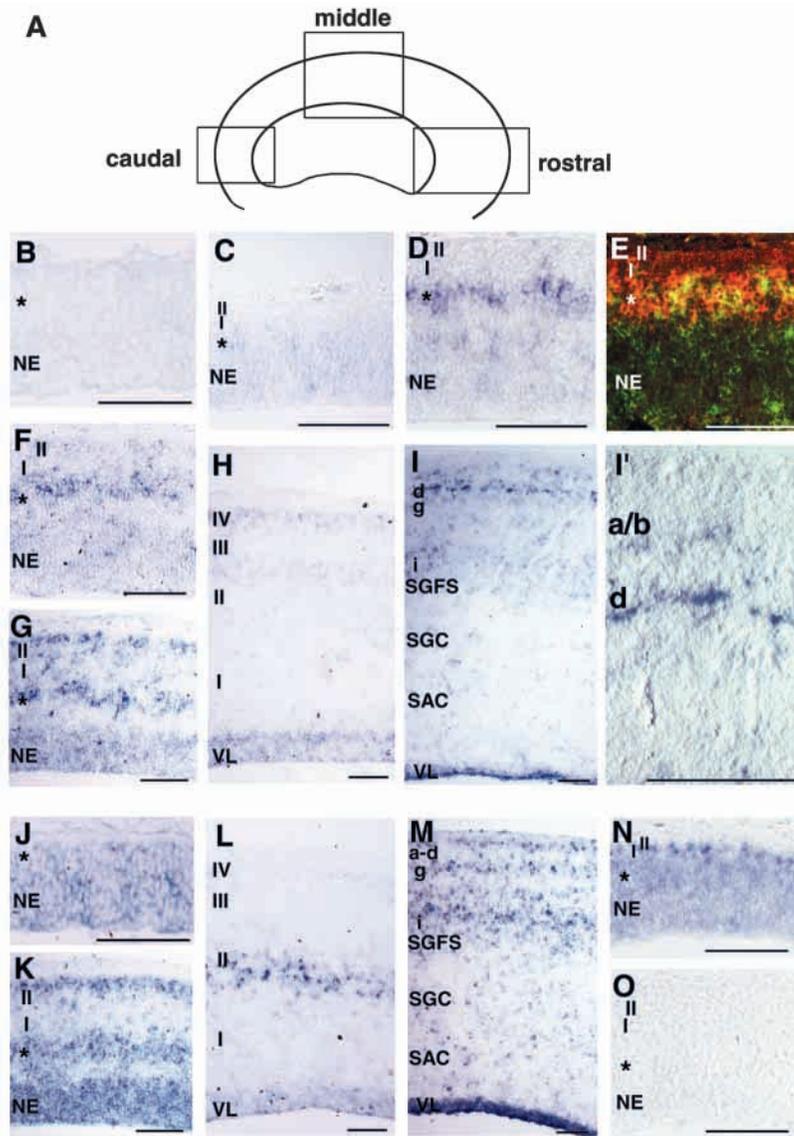

Fig. 2. Expression of *Grg1*, *Grg4* and En2 in developing chick tecta. (A) Approximate position of the figures. (B-I) In situ hybridization for *Grg4*: (B) E4 (stage 22), (C,D) late E5 (stage 28, C at the caudal and D at the rostral), (E,F) E6 (stage 29, E at the caudal and F at the middle, E shows immunohistochemistry with anti-Hu-C/D in red and in situ hybridization for *Grg4* in green), (G) late E6 (stage 30), (H) E8 (stage 34) and (I) E14 (stage 40). I' is higher magnification of I. (J-M) In situ hybridization for *Grg1*: (J) E4 (stage 22), (K) late E6 (stage 30), (L) E8 (stage 34), (M) E14 (stage 40). (N,O) Immunohistochemistry with anti-En2 antibody at late E5 (stage 28; N, caudal; O, rostral). *Grg4* is not expressed at late E3 (B). Its expression resumes at late E5 in a gradient along rostrocaudal axis; rostral high (D) and caudal low (C). *Grg4* is expressed in the neuroepithelium (NE) and in the Hu-C/D-positive early neuronal layer (∗). At late E6.5, *Grg4* expression is observed in laminae II and I (F,G). Expression in the ventricular layer (VL) is still observed at stage 40 (I). *Grg1* is continuously expressed in the ventricular layer to E14 (J-M). En2 is expressed at late E5 in an opposite gradient to *Grg4*: caudal high (N) and rostral low (O). Scale bars: 100 μm.

early neurons that are waiting to migrate. At the central part of the tectum at E6 (stage 29), *Grg4*-expressing cells were detected in the ventricular layer and in laminae II and I (Fig. 2F). The intensity and the number of *Grg4*-expressing cells were increased at E6.5 (stage 30, Fig. 2G). Expression in the ventricular layer continued to E14 (stage 40, Fig. 2H,I). Expression in laminae II and I was weakened after E7 (stage 31). At E8 (stage 34), *Grg4* expression was only slightly

observed in the upper laminae (Fig. 2H), while at E14 (stage 40), *Grg4* expression was observed in lamina d of the SGFS (Fig. 2I, I′).

We also examined the expression pattern of *Grg1*. *Grg1* was continuously expressed in the ventricular layer from E2 to E14 (Fig. 2J-M). Expression was visible throughout the whole mantle layer before late E6 (stage 30, Fig. 2K), but was restricted to the deeper lamina II by E8 (stage 34, Fig. 2L). Its
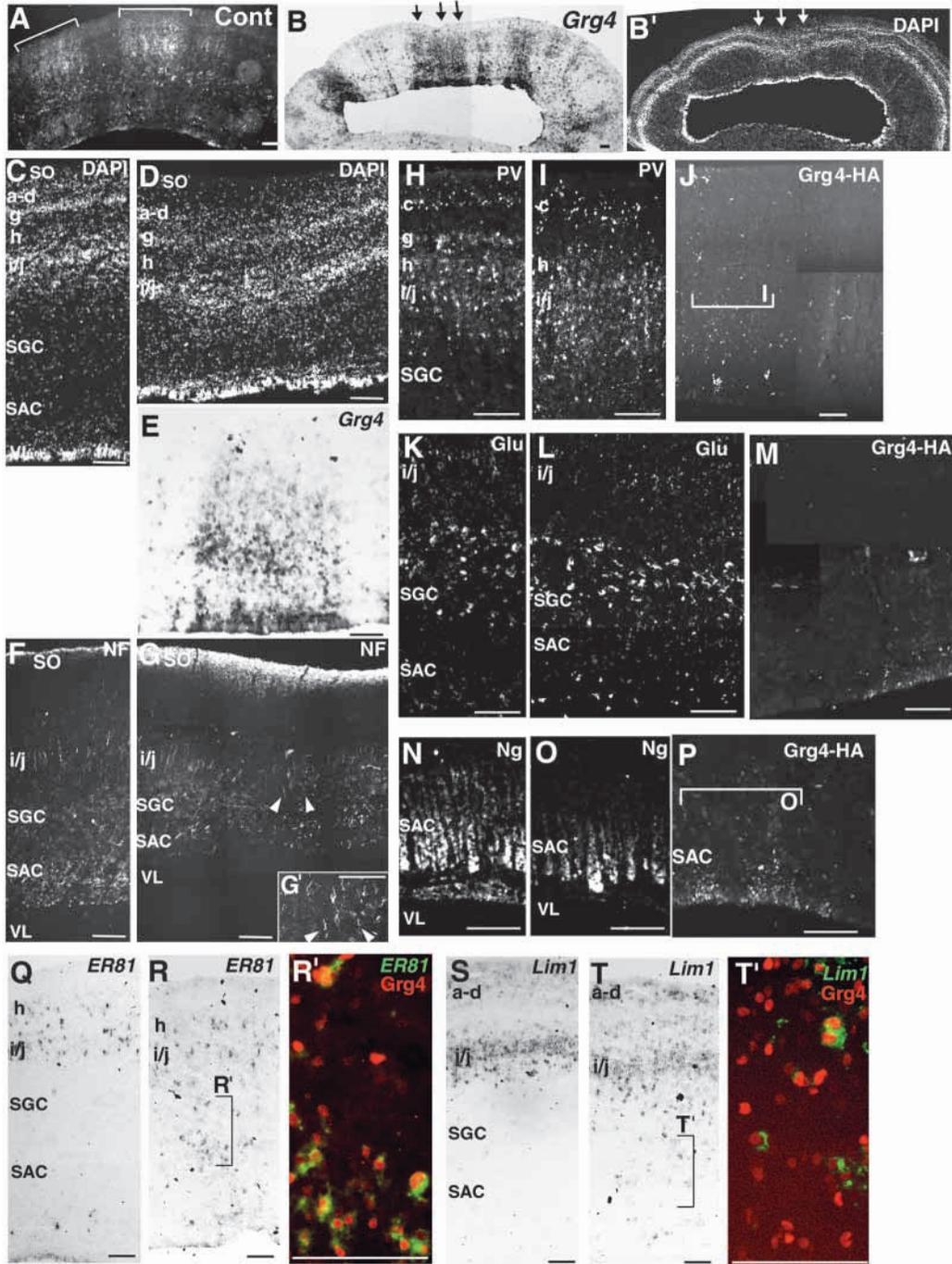
Fig. 3. Effects of *Grg4* misexpression on tectal laminar formation. (A-G) Tecta at E12. (A) Low-power micrograph of an RCAS-AP-misexpressing tectum, which served as the control. Immunohistochemistry is with anti-gag antibody. The transfection sites are indicated by brackets. (B,B′) RCAS-*Grg4*-misexpressing tectum. In situ hybridization for *Grg4* (B) and DAPI staining (B′). (C,D) DAPI staining of the control (C) and *Grg4*-misexpressing (D) tecta. (E) Higher magnification of *Grg4* expressing site in E. (B,B′,D,E,G) are from adjacent sections of the same tectum. On B and B′, the site that corresponds to D and E is indicated by arrows. (F,G) Immunohistochemistry with anti-neurofilament antibody on the control (F) and *Grg4*-misexpressing tecta (G). (H-T) E14 tecta. Immunohistochemistry with anti-PV (H,I), anti-Glutamate (K,L) and anti-NgCAM antibodies (N,O). In situ hybridization for *ER81* (Q,R) and for *Lim1* (S,T). Merged figures of Grg4 and *ER81* (R′) and Grg4 and *Lim1* (T′) at the site indicated by brackets on R and T, respectively. *Grg4* misexpression was assessed immunohistochemically with antibody against the HA tag (J,M,P,R′,T′). Control (H,K,N,Q,S) and *Grg4*-misexpressing site (I,J,L,M,O,P,R,T). L and M are the same field of the same section. *Grg4* expressing site is indicated in L. In *Grg4*-misexpressing regions, lamina g seemed to be reduced (D), but lamina i/j was increased (D,G). Arrowheads in G indicate radial neuronal fibers. Expression of PV (H) indicates that lamina g is specifically disrupted by *Grg4* misexpression (I). Cells that express glutamate in SGC and SAC are reduced at the Grg4-misexxpressing site (right hand side of L, where Grg4 misexpressing site is indicated as Grg4). *ER81* and *Lim1*, which are normally expressed in lamina i/j, are expressed in deeper layers in the *Grg4*-misexpressing region (Q-T). Scale bars: 100 μm for A-T; 20 μm for G′.

expression was again visible within entire laminae by E14 (stage 40, Fig. 2M).

En2 expression was detected at late E5 (stage 28) in an opposite gradient to that of *Grg4*: rostral low and caudal high (Fig. 2N,O). En2 expression then disappeared from the rostral side, being completely absent by E7 (stage 31).

Effect of *Grg4* misexpression on tectal lamination

As the reappearance of *Grg4* expression and the change in migration pattern of postmitotic cells occur at late E5 (stage 28), we suspected that *Grg4* might be responsible for the fate change of the postmitotic cells. We carried out misexpression of *Grg4* by in ovo electroporation, in which proviral plasmid vector that contained RCAS-Grg4 (Hughes et al., 1987) was electroporated into virus-sensitive embryos at E2 (stage 9-11). As a control, proviral plasmid that contained RCAS-AP was also electroporated. Misexpression in the neuroepithelium expands by secondary infection with the retrovirus in virus-sensitive embryos (Fig. 3A,B). At E12, in the RCAS-AP-infected tecta,13 laminae [SO, SGFS (a-d, g-j), SGC, SAC and the ventricular layer] were clearly distinguished by staining with DAPI (Fig. 3A,C) and with anti-neurofilament antibody (Fig. 3F), as is seen in tecta without any treatment. In RCAS-Grg4-infected tecta, the tectal wall was thinner at the *Grg4*-misexpressing region (*n*=4/4, Fig. 3B). DAPI staining showed that lamina g of the SGFS became inconspicuous, suggesting that the cells that normally form this structure were halted in their migration (Fig. 3D). However, lamina i/j of the SGFS increased in thickness, indicating that more cells migrated into lamina i/j than in the control (Fig. 3D). Immunohistochemistry with anti-neurofilament antibody showed that the SAC and SGC were thinner than those in the controls, and that radial neuronal fibers in lamina i/j invaded the deeper lamina that corresponds to the SGC (Fig. 3G,G′).

Next, we looked at the effects on genes that are specifically expressed in the laminae at E14. Parvalbumin (PV) is a Ca^{2+}-binding protein in GABAergic neurons and is normally expressed in cell somata and fibers of laminae a-c, g, h and i/j of the SGFS (Fig. 3H). Within the *Grg4*-misexpressing region, PV-positive cells were detected in lamina a-c, h and i/j, but were not detected in lamina g (Fig. 3I). In the control region, glutamate was detected in the large cells of the SGC (Fig. 3K), and Ng-CAM was detected immunohistochemically in axonal bundles of the SAC (Fig. 3N), as reported previously (Kröger and Schwarz, 1990; Yamagata et al., 1995). The number of glutamate-positive cells was reduced in the *Grg4*-misexpressing region (right hand side of Fig. 3L), and the region of Ng-CAM-positive bundles in the SAC was diminished (Fig. 3O).

In the control, transcription factors *ER81* and *Lim1* are expressed mainly in the laminae that are composed of late migratory cells; *ER81* in laminae h and i/j of the SGFS and *Lim1* in laminae i/j of the SGFS (Fig. 3Q,S). Weak expression of *Lim1* was also seen in laminae a-d of SGFS (Fig. 3S). When *Grg4* is misexpressed, *ER81* and *Lim1* expression is also seen in the laminae that correspond to the SGC and SAC (Fig. 3R,T), where cells that express *ER81* or *Lim1* always misexpressed *Grg4* (Fig. 3R′,T′). These *ER81*- and *Lim1*-positive cells in the deep laminae may have acquired the property of one of the laminae h-j. In other words, laminae h-j may have been enlarged, even admitting that some of the
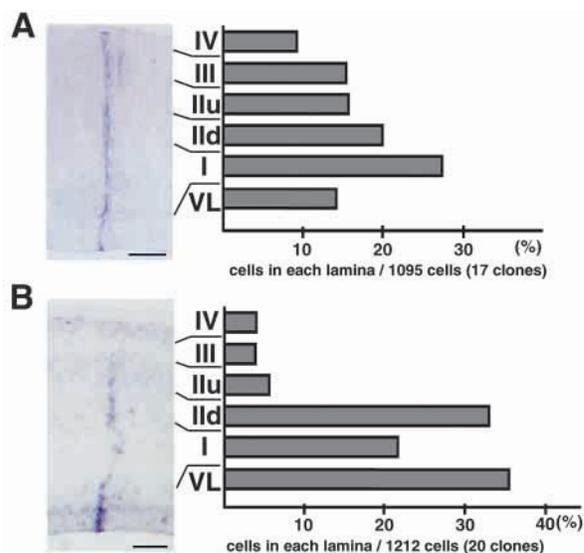

Fig. 4. Clonal analysis of the migration of *Grg4*-expressing cells. (A) Electroporation with RCAS-AP on virus-resistant embryos at E2 that were fixed at E8. (Left column) AP immunocytochemistry. (Right column) Number of AP-positive cells in each lamina. (B) Electroporation with RCAS-Grg4 on virus-resistant embryos at E2 that were fixed at E8. (Left column) In situ hybridization for *Grg4*. (Right column) Number of *Grg4*-expressing cells in each lamina. In virus-resistant embryos, misexpression is limited to the descendents of originally transfected cells. AP-positive cells are present throughout all laminae (A), but *Grg4*-expressing cells are found mainly in lamina IId (B). Scale bars: 100 μm.

ER81- and *Lim1*-positive cells in deep laminae are still en route to their destination. In total, nine embryos were sacrificed at E14, and above mentioned effects were found in seven embryos.

The results suggest that *Grg4* instructs postmitotic neuronal cells to behave as late migratory cells. Consequently, lamina g, which is formed by early migratory cells, disappears, while laminae h-j, that are formed by late migratory cells, become enlarged.

Grg4 changes the fate of early migratory cells to late migratory cells

Our results indicated that *Grg4* switched the fate of the early migratory cells to that of late migratory cells. We confirmed this by electroporation of retroviral vector into virus-resistant embryos at E2 (stage 9-10), where misexpression is limited to the descendents of originally transfected cells. By E8 (stage 34), after electroporation with the RCAS-AP vector, a lineage of transfected cells was distributed radially throughout the tectal wall (Fig. 4A). Quantitative examination was carried out on 17 clones from six embryos, and showed that the cells were almost equally distributed in each lamina (Fig. 4A). However, after electroporation with RCAS-Grg4 (20 clones from eight embryos), the *Grg4*-expressing cells were concentrated in the deeper lamina II that is composed of late migratory cells (Fig. 4B). The labeled cells in lamina I may be those en route to their final destination. This result indicates that *Grg4* directly governs the neural precursor cells to take the late migratory fate.
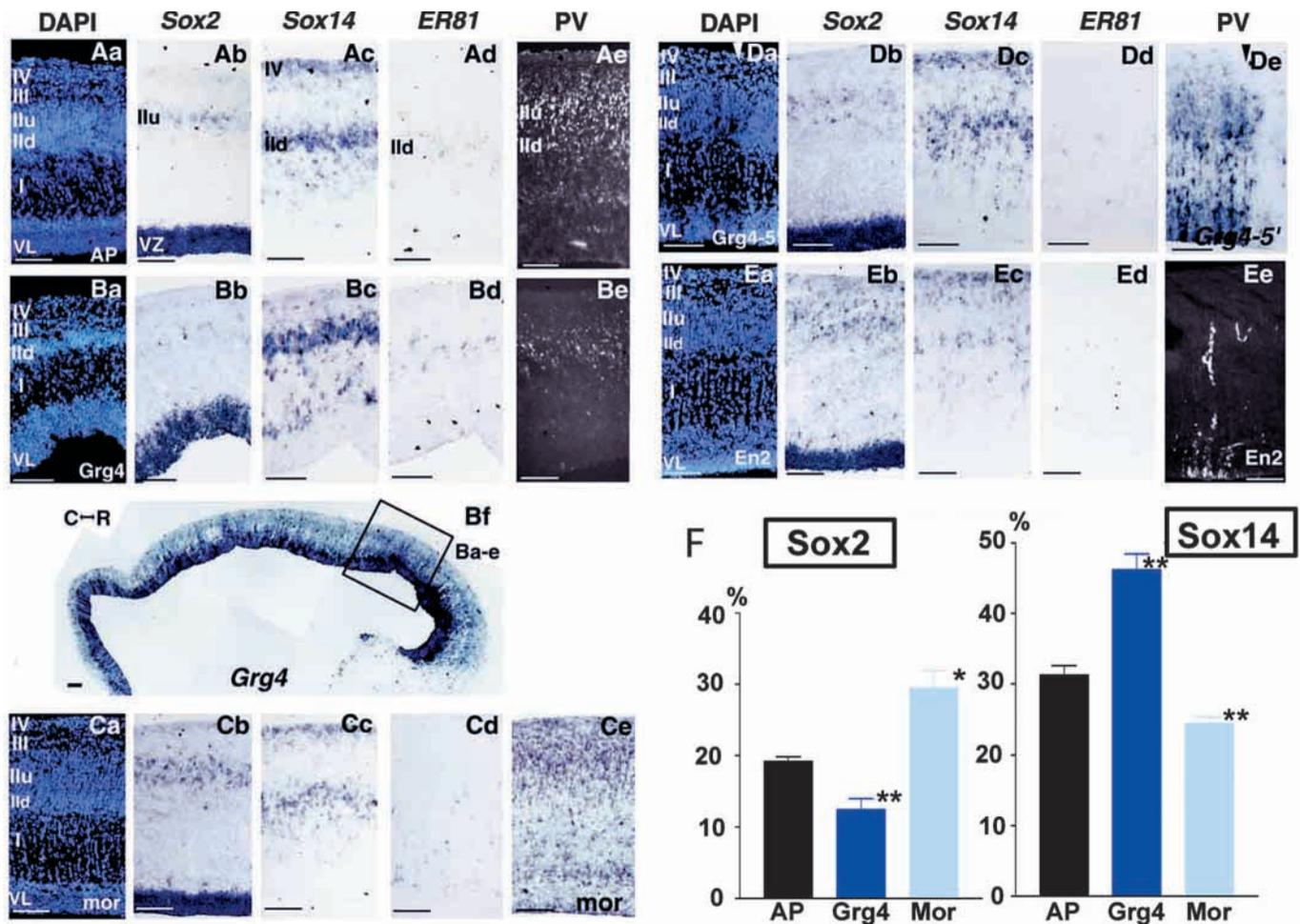
Fig. 5. *Grg4* instructs the tectal postmitotic cells to take a late migratory pathway. (A) Control E8 tecta in which RCAS-AP was electroporated at E2. (B) *Grg4* misexpression by RCAS-Grg4. (C) Application of morpholino antisense oligonucleotide for *Grg4* at E5. (D) *Grg4-5′* misexpression by RCAS-Grg4-5′. (E) En2 misexpression by RCAS-En2 infection. (F) Relative cell numbers of Sox2- and Sox14-positive cells. In A-E: (a) DAPI staining, (b) in situ hybridization for *Sox2*, (c) in situ hybridization for *Sox14*, (d) in situ hybridization for *ER81*. (A, part e; B, part e) Immunostaining for PV. (B, part f) Low-power micrograph to show *Grg4* misexpression. (C, part e) immunostaining for FITC to show FITC-conjugated morpholino. (D, part e) Immunostaining for HA Tag. Immunostaining for En2. In the control (A), *Sox2* is expressed in lamina IIu and the ventricular layer (VL). *Sox14* is expressed in laminae IV and IId. *ER81* is expressed specifically in lamina IId. PV is expressed in laminae III-II at E8. In the *Grg4*-misexpressing region, reduction of lamina I, IIu and IV is assessed from the expression of *Sox2*, PV and *Sox14* (B, part a-c; B, part e). Treatment with morpholino antisense oligonucleotide for *Grg4* exerted reverse effects: expansion of lamina IIu (C, part b), reduction of lamina IId (C, parts c,d). *Grg4-5′* acted as a dominant-negative form for *Grg4*; expansion of lamina I and IIu (D, part b), reduction of lamina IId (D, parts c,d). En2 misexpression also resulted in the reverse effects to *Grg4*: expansion of lamina IIu (E, part b), reduction of lamina IId (E, parts c,d). For quantification, percent of *Sox2*- and *Sox14*-positive cells around the lamina II in total cells of mantle layer was calculated (F). The number of cells in a rectangle, one side of which is 100 μm and parallel to the ventricular surface, was counted on four samples from two embryos each. The graph shows that Grg4 forces tectal postmitotic cells to follow a late migratory pathway. Error bars represent s.e.m. Asterisks indicate significant differences from the control (single asterisk, $P<0.05$; double asterisks, $P<0.005$). AP, control *AP*-transfected tecta; Grg4, *Grg4* misexpressing tecta; Mor, tecta treated with morpholino antisense oligonucleotide. Scale bars: 100 μm.

The notion that *Grg4* instructs the neuroepithelial cells to take late migratory fate was further confirmed by looking at the effects on other marker molecules. We have shown that laminae IV-III, upper lamina II and lamina I of E8 tecta are mainly composed of early migratory cells, and that deeper lamina II is mainly composed of late migratory cells. In the control tecta, *Sox2* was expressed in upper lamina II and the ventricular layer (Fig. 5A, part b) and *Sox14* was expressed in lamina IV and deeper lamina II (Fig. 5A, part c). *ER81* was expressed in deeper lamina II. (Fig. 5A, part d). Parvalbumin

(PV) was intensely expressed in upper lamina II and weakly expressed in lamina III and deeper lamina II (Fig. 5A, part e).

In the *Grg4*-misexpressing region, the laminae composed of early migratory cells were specifically reduced ($n=13/13$, Fig. 5B, parts a-f). The number of cells in lamina I was reduced (Fig. 5Ba), and *Sox2*-positive and PV-positive cells in the upper lamina II almost disappeared (Fig. 5B, parts b,e). In terms of *Sox-14* expression, lamina IV was nearly absent, in contrast to the control tectum (Fig. 5B, part c). However, *Sox14*-positive and *ER81*-positive cells in deeper lamina II, which is composed

of late migratory cells, were rather increased compared to the control (Fig. 5B, parts c,d). The effects of *Grg4* on molecular markers within each lamina indicate that *Grg4* had changed the fate of early migratory cells to that of late migratory cells.

Inhibition of Grg4 function

To further investigate the ability of *Grg4* to direct the fate of neuronal precursor cells we carried out experiments using morpholino antisense oligonucleotide (Heasman et al., 2000). The antisense oligonucleotide was applied by electroporation at E5 (stage 28), the stage that coincides with *Grg4* re-expression (Fig. 5C, parts a-e). Control morpholino oligonucleotide did not affect laminar formation when observed at E8 (data not shown). *Grg4* antisense morpholino oligonucleotide increased the number of *Sox2*-positive cells in upper lamina II by E8, which is mainly composed of early migratory cells (Fig. 5C, part b). However, the number of *Sox14*-positive and *ER81*-positive cells in deeper lamina II was decreased (Fig. 5C, parts c,d). Expansion of upper lamina II and reduction of deeper lamina II (n=5/7) is the opposite result to that obtained with *Grg4* misexpression. As deeper lamina II is mainly composed of late migratory cells, we postulate that the *Grg4* morpholino antisense oligonucleotide may have prevented the neuronal precursor cells from acquiring a late migratory fate.

In our previous study (Sugiyama et al., 2000), it was shown that *Grg4* repressed En2 expression, and that the 5′ region of *Grg4* (*Grg4-5′*) induced En2 expression in the tectum. In other words, *Grg4-5′* acts as a dominant-negative form of *Grg4* in tectum development. When we misexpressed *Grg4-5′* by electroporation with RCAS-*Grg4-5′*, the results were similar to those obtained after *Grg4* morpholino antisense oligonucleotide application (n=3/4, Fig. 5D, parts a-d). *Sox2*-positive cells in upper lamina II was increased (Fig. 5Db), and the expression of *Sox14* and *ER81* in deeper lamina II was weakened (Fig. 5D, parts c,d). Laminae IV-III and the ventricular layer were not affected by *Grg4-5′*. A remarkable feature was that deeper lamina II was reduced and lamina I extended to lamina II (Fig. 5D, parts a-e).

En2 is expressed in a gradient along the rostrocaudal axis from E2 (Gardner et al., 1988). The gradient of En2 was opposite to that of *Grg4* at E5 (stage 28, Fig. 2N,O). *Grg4* could repress the expression of En2 (Sugiyama et al., 2000), and continued misexpression of *En2* resulted in retardation of laminar formation (Logan et al., 1996). We misexpressed *En2* by infection with RCAS-En2 viral fluid at E2 (stage 8-9). *En2* misexpression exerted similar effects as treatment with *Grg4* morpholino antisense oligonucleotide or misexpression of *Grg4-5′* (n=2/2). In the En2-misexpressing region of the E8 tectum, the number of *Sox2*-positive cells in upper lamina II was increased (Fig. 5E, parts a,b) and the number of *Sox14*-positive and *ER81*-positive cells in deeper lamina II was decreased (Fig. 5E, parts c,d). The results indicate that misexpression of En2 may restrict neuronal precursor cells to an early migratory fate.

Quantification of *Sox2*- and *Sox14*-positive cells

It was indicated that Grg4 forced the cells to follow late migratory pathway. We confirmed the notion by quantification on E8 embryos. At E8, deeper lamina II consists of late migratory cells, and upper lamina II consists of early migratory cells. *Sox2* and *Sox14* are good markers for deeper lamina II and upper lamina II, respectively (Fig. 5A, parts a,c). For quantification, a rectangle that covers whole the wall of the tectum (one side of the rectangle is 100 μm and parallel to the ventricular surface) was made on the Photoshop image. The number of *Sox2*- or *Sox14*-positive cells around lamina II and the number of total cells in the mantle layer were counted on four samples from two embryos each. Percentage of Sox2- or Sox14-positive cells was calculated. According to our expectation, percentage of *Sox2*-positive cells, which are early migratory cells, was reduced after *Grg4* misexpression (19.17±7.2% s.e.m. in controls, and 12.15±1.52% in *Grg4* misexpressing tecta, n=4 for each, Fig. 5F). However, treatment with morpholino antisense oligonucleotide for *Grg4* increased the percentage of Sox2-positive cells (29.42±2.46%, n=4, Fig. 5F).

Percentage of Sox14-positive cells, which are late migratory cells, was increased in the *Grg4* misexpressing tecta (31.33±1.26% in controls, and 46.24±2.14% in *Grg4* misexpressing tecta, n=4 for each, Fig. 5F). The percentage of Sox14-positive cells was reduced after treatment of morpholino antisense oligonucleotide for *Grg4* (24.49±0.88%, n=4, Fig. 5F).

Quantitative analyses clearly show that Grg4 forces neuronal precursor cells to follow late migratory pathway.

Effect of the *Grg* family on tectal neuronal precursors

Another *groucho*-related gene, *Grg1*, is continuously expressed in ventricular cells from E2 and we wondered if this gene could influence laminar formation of the tectum. Electroporation with the RCAS-Grg1 expression vector was carried out at E2. In *Grg1*-misexpressing regions, the number of *Sox2*-, *Sox14*- and *ER81*-expressing cells was decreased throughout laminae IV-I (n=5/5, Fig. 6A, parts a-d).

Drosophila Groucho and human *TLE1*/*Grg1*, were shown to inhibit transcription of the genes for neuronal differentiation (Paroush et al., 1994; Fisher et al., 1996). We looked at effects of *Grg1* and *Grg4* misexpression on the expression of the proneuronal marker gene, *Cash1*. *Cash1* is a chick *achaete-scute* homolog, and is one of the targets for Gro/Grg (reviewed by Kageyama and Nakanishi, 1991). In the control E8 tecta, *Cash1* expression was detected in the upper ventricular layer (Fig. 6B). In the *Grg1*-misexpressing region, *Cash1* expression was repressed in the ventricular layer (Fig. 6C), indicating that *Grg1* prevents ventricular cells from expressing neuronal genes, in accordance with previous studies (reviewed by Fisher and Caudy, 1998; Yao et al., 2000). In the *Grg4*-misexpressing region, however, *Cash1* expression was expanded in the ventricular layer, compared with the control (Fig. 6D). Double-staining for Hu-C/D and *Grg4*-HA showed that many *Grg4*-misexpressing cells gathered at the boundary between lamina I and the ventricular layer (Fig. 6E), where these cells did not incorporate BrdU (Fig. 6F,G). These results indicate that *Grg4* does not inhibit ventricular cells from neuronal differentiation, but forces postmitotic cells to acquire a late migratory fate.

Disruption of retinotectal projection by *Grg4*

Retinotectal projection is organized in a precise retinotopic manner. Retinal axons run tangentially on the tectal surface to
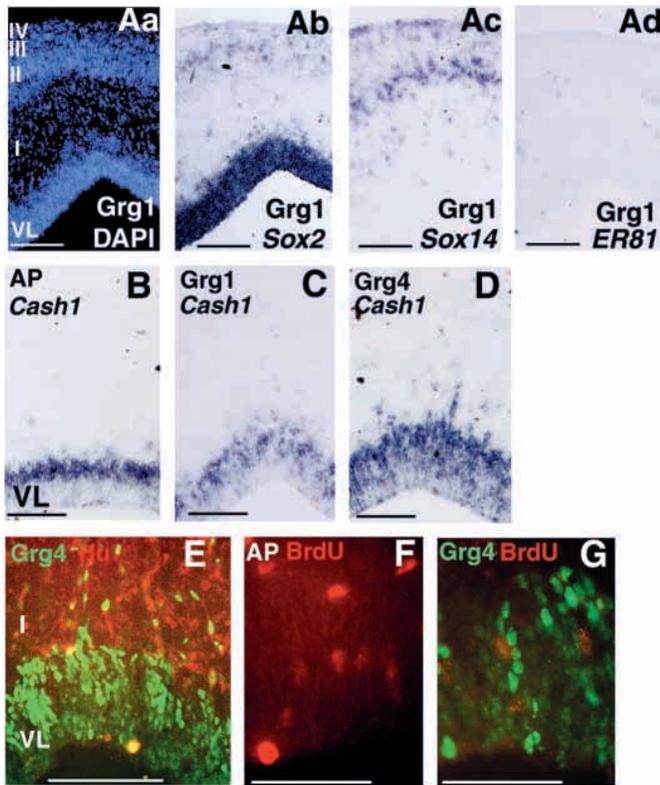
Fig. 6. *Grg1* restricts cells to the neuroepithelial layer. (A) DAPI staining (a), and in situ hybridization for *Sox2* (b), *Sox14* (c) and *ER81* (d) in Grg1-misexpressing E8 tecta visualized using by RCAS-Grg1. (B-D) In situ hybridization for *Cash1* in E8 tecta that were transfected with RCAS-AP (B), RCAS-Grg1 (C) or RCAS-Grg4 (D). (E) Immunostaining for Grg4-HA in green and Hu-C/D in red. (F,G) Immunostaining for HA in green and BrdU in red in E8 tecta that were transfected with RCAS-AP (F) or RCAS-Grg4 (G). *Cash1* is expressed in the ventricular layer (VL, B). In the *Grg1*-misexpressing region, *Cash1* expression is repressed (C) so that all laminae (IV-I) are incompletely formed on E8 tecta (A). In the *Grg4*-misexpressing region, expansion of the ventricular layer by postmitotic neuronal precursors is observed (D,E,G). Scale bars: 100 μm for A-E; 50 μm for F,G.

form the SO and make a right turn to arborize in laminae a/b, d and e/f of the SGFS (LaVail and Cowan, 1971a; Crossland et al., 1974; Rager and von Oeyhausen, 1979; McLoon, 1985; Thanos and Bonhoeffer, 1987; Yamagata and Sanes, 1995). They do not normally invade lamina g. We showed that lamina g was mainly composed of early migratory cells and that it was disrupted by *Grg4* misexpression. Thus, we were interested in the behavior of retinal axons in the absence of lamina g. All axons emanating from a retina were labeled by injecting the eye with a solution of HRP at E15, or a small group of axons was labeled by placing a crystal of DiI on the retina at E15. The embryos were fixed at E17, when remodeling of the retinal axons was complete (Nakamura and O'Leary, 1989). At E17, when remodeling of retinal fibers is complete (Nakamura and O'Leary, 1989), retinal axons in normal tecta were restricted to the retinorecipient laminae superficial to the border between lamina f and g (Fig. 7A). In eight out of 11 RCAS-Grg4-infected tecta, terminal arbors invaded deeper, beyond the disrupted lamina g (Fig. 7B). The regions of the tecta in which retinal axons penetrated deep to lamina g were positive for the viral gag protein, indicating the presence of virus carrying the Grg4 gene (Fig. 7C).

We were then interested in the behavior of arbors in their initiation phase, and cryosections of E12 tecta were stained immunohistochemically with anti-neurofilament antibody. The SO, which consists of retinal axons, was stained heavily in both the control and *Grg4*-misexpressing region (Fig. 7D,E). Some fibers were branching directed inside the tectum. These fibers may be terminal arbors in their initial phase. In the control region, terminal arbors do not invade lamina g, in contrast to the *Grg4*-misexpressing region in which terminal arbors were able to reach lamina h.

DISCUSSION

We have shown by *lacZ* transfection that the migration pattern for tectal postmitotic cells is different between those that leave before E5 (early migratory cells) and those that leave after E5 (late migratory cells). A
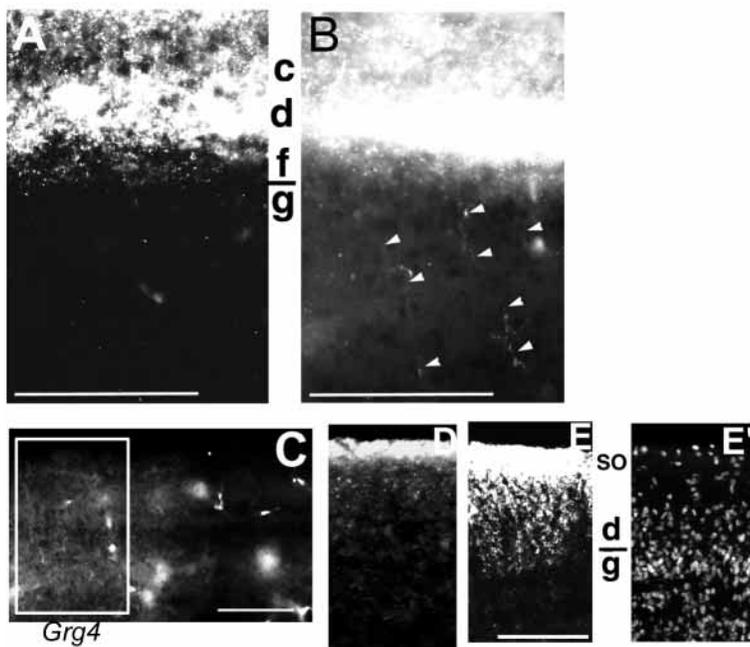
Fig. 7. Disruption of retinotectal projection by *Grg4*. (A,B) Terminal arborizations in the control (A) and *Grg4*-misexpressing region (B). HRP was injected in the contralateral eye at E15, the tectum was fixed at E17, and fibers were visualized with anti-HRP antibody on the slice. (C) *Grg4* misexpression was assessed by immunohistochemical staining with anti-gag antibody on the same slice as B. In the control tectum, retinal fibers arborize superficial to lamina g (A), but in the *Grg4*-misexpressing tectum, retinal axons pass deeper beyond lamina g (arrowheads in B). The rectangle on C indicates approximate area of B. (D,E,E′) Immunostaining with anti-neurofilament (D,E) and DAPI staining (E′) on the sagittal section of the control (D) and *Grg4*-misexpressing region (E) on E12 tecta.

transcriptional repressor *Grg4* is expressed after E5 (stage 28) in the ventricular layer. Misexpression of *Grg4* resulted in disruption of lamina g of the SGFS, which is composed of early migratory cells, and in the expansion of laminae composed of late migratory cells. Morpholino antisense oligonucleotide for *Grg4* and the expression of Grg4-5′ and En2 exerted reverse effects. Finally, in the absence of lamina g, retinal arbors aberrantly invaded non-retinorecipient laminae.

Migration of the postmitotic cells in the tectum

The migration of postmitotic cells from the ventricular layer to their destination, is dependent on their time of birth (LaVail and Cowan, 1971b; Gray et al., 1988; Gray and Sanes, 1991). We have shown here that two migratory groups, designated as early and late migratory cells, contribute to tectal architecture: the first group leaves before E5 and the second group leaves after E5. Early migratory cells form laminae a-g of the SGFS, SGC, SAC, SGP and SFP, while late migratory cells form laminae h-j of the SGFS. LaVail and Cowan (LaVail and Cowan, 1971b) reported that there are three migration waves of postmitotic cells that contribute to tectal laminar formation. The first-born neurons form the SGC, SAC, SGP and SFP; and the second-born neurons formed laminae a-g of the SGFS. These first and second waves mostly occur before E5 in a chronologically overlapping manner. The third wave occurs between E6 and E8, and forms laminae h-j of the SGFS. Thus, these first and second waves may correspond to the early migration in our study, and the third wave may correspond to the late migration.

Many young neurons of the early migratory group first accumulate over the neuroepithelium, later migrating to establish laminae II and I by E6 (see Fig. 1) (Gray and Sanes, 1991). Late migratory cells remain in the ventricular layer up until E6, subsequently migrating to intervene between laminae II and I by E8. As a result, in E8 tecta, the upper laminae (lamina IV to upper lamina II) and the deeper lamina (lamina I) consist of early migratory cells, and the intervening lamina (deeper lamina II) consists of late migratory cells. Thus, we propose that lamina II actually consists of two divisions: upper lamina II and deeper lamina II. As most neuronal precursors that form tectal laminae are postmitotic by E8 (LaVail and Cowan, 1971b), the five laminae of E8 become reorganized into 13 laminae by E12. Early migratory cells stay in upper laminae (laminae a-g of the SGFS) and deeper laminae (SGC, SAC, SGP and SFP). It must be emphasized that lamina g was mostly composed of early migratory cells (see Fig. 3H). The contribution of late migratory cells to lamina g is minimal (see Fig. 3J). Late migratory cells were mainly found in laminae h-j of the SGFS. Comparison of late migratory cells at E8 and E12 indicates that deeper lamina II at E8 may become reorganized into laminae h-j of the SGFS by E12.

Role of *Grg4* in directing the fate of tectal postmitotic cells

As discussed above, the fate of postmitotic cells changes after E5. As *Grg4* is re-expressed at E5 and continues thereafter in the tectal ventricular layer, we suspected that *Grg4* might be responsible for the fate change of the tectal postmitotic cells. As expected, *Grg4* misexpression resulted in a reduction in thickness and cell number of upper and deeper laminae of E8 tecta that are composed of early migratory cells. Conversely,

the intervening middle lamina (deeper lamina II), which is composed of late migratory cells, was rather increased by E8. Quantitative analysis clearly showed that the percent of cell number in deeper lamina II was increased, but that in upper lamina II was decreased (see Fig. 5F). At E14, the middle laminae (laminae h-j of the SGFS), which are composed of late migratory cells, expanded, whereas upper (lamina g of SGFS) and deeper (SGC-SFP) laminae were reduced. Disruption of lamina g was distinct. This result is explained by the fact that lamina g is mostly composed of early migratory cells (see Fig. 1I,J), and supports the idea that *Grg4* confers a late migratory fate to tectal postmitotic cells. This was further confirmed by clonal misexpression of *Grg4*. We could limit the misexpression to the descendents of the originally transfected cells by carrying out electroporation with proviral plasmid vectors on virus-resistant embryos. Clonal misexpression of AP showed that the AP-positive cells radially spanned between the ventricular and pial surfaces (Gray et al., 1988; Gray and Sanes, 1991), whereas clonal misexpression of *Grg4* showed that the *Grg4*-misexpressing cells were mainly restricted to the intervening middle lamina (deeper lamina II). *Grg4*-misexpressing cells were also found in the deeper laminae (lamina I and the early neuronal layer), where they may still be en route to their ultimate destination.

If *Grg4* does indeed instruct tectal postmitotic cells to follow the late migratory pathway, blockade of *Grg4* should exert reverse effects. Accordingly, application of *Grg4* morpholino antisense oligonucleotide at E5 (stage 28) resulted in a decrease the number of late migratory cells and in the thickness of the corresponding laminae. On the contrary, the number of early migratory cells increased. The expression of *Grg4*-5′ has been shown to exert dominant-negative type effects (Sugiyama et al., 2000). In our hands, misexpression of *Grg4*-5′ exerted similar effects as that of the *Grg4* morpholino antisense oligonucleotide. These results support the idea that *Grg4* instructs tectal postmitotic cells to follow a late migratory pattern.

Grg1 is continuously expressed from E2 to E14. *Drosophila* Groucho and human TLE1/Grg1 can inhibit transcription of neuronal genes (Paroush et al., 1994; Fisher et al., 1996) and Grg1 can keep neuroepithelial cells in an undifferentiated proliferative state (Yao et al., 2000). This study also showed that *Grg1* could repress the generation of neuronal precursor cells, resulting in poor differentiation of the tectal laminae. We concluded that the effects of *Grg4* do not result from suppression of neuronal differentiation but from the conversion of early migratory cells into late migratory cells.

The molecular events involved in deciding the fate of progenitor cells in the ventricular layer of the spinal cord have been studied in detail (reviewed by Jessell, 2000). Recent studies indicate that the interactions of certain homeodomain (HD) and bHLH proteins defined the neuronal subtype identity (Pierani et al., 2001; Vallstedt et al., 2001; Mizuguchi et al., 2001; Novitch et al., 2001). Gro/Grg-mediated transcriptional repression probably plays a role in regulation of the spatiotemporal expression of the homeodomain proteins in progenitor cells (Muhr et al., 2001). In laminar formation of the cerebral cortex, cell fate is decided in the ventricular layer before the progenitor cells reach their destination (McConnell, 1988), although candidate molecules have not yet been identified. Our results showed that *Grg4*-

expressing postmitotic cells followed the late migratory pathway, and we propose that *Grg4* directs the fate of these cells to follow the late migratory fate in tectal laminar formation.

In normal development, En2 expression (caudal high and rostral low) is in an opposite gradient to *Grg4*. The second phase of *Grg4* expression (after E5) commences at the rostral side of the tectum, and proceeds to the caudal side. Thus, postmitotic cells at the rostral part of the tectum may acquire a late migratory fate earlier than those at the caudal part. This is reflected in the cytoarchitectural development of the tectum, with the rostral part proceeding faster than the caudal. En2 expression may force the ventricular cells to take an early migratory fate.

Lamina g of the SGFS functions as a barrier for the terminal retinal arbors

The projection of retinal axons in retinorecipient tectal laminae has been described in previous studies (Crossland, 1974; Rager and von Oeyhausen, 1979; McLoon, 1985; Thanos and Bonhoeffer, 1987). Retinal axons enter the tectum from the rostral part and run caudally at the most superficial layer to form the SO. Axons make a right turn to make terminal arborizations in lamina a-f of the SGFS at their target zone. Temporal retinal fibers make terminal arborizations at the rostral part of the tectum, but not before first extending beyond the target to the central part of the tectum, where they can even make arborizations even outside of the target area. Arborizations outside of the target zone are pruned and become confined to the definitive target zone by E16 (Nakamura and O'Leary, 1989). Within the target zone, retinal arbors reach lamina f of the SGFS (LaVail and Cowan, 1971a), but never pass through lamina g. In the *Grg4*-misexpressing regions, where lamina g of the SGFS was disrupted, retinal axons were seen to extend beyond lamina g, which may express a non-permissive signal (Yamagata and Sanes, 1995). Our preliminary results indicated that refinement of retinal projections was also disturbed in the *Grg4*-misexpressing region. It has been proposed that synchronized firing of the neighboring fibers plays an important role in refining the retinal projection (O'Leary et al., 1986; Stryker and Harris, 1986; Cline et al., 1987; Kobayashi et al., 1990; Meister et al., 1991; Mooney et al., 1996), and that maturation of GABAergic inhibitory neurons is important for activity-dependent refinement in the visual cortex (Fagiolini and Hensch, 2000). In the tectum, parvalbumin, which is expressed in GABAergic neurons, is expressed in lamina g. Thus, there is a possibility that lamina g is involved in refinement of the retinotectal projection. In conclusion, lamina g of the SGFS may play important roles in the formation of the topographic retinotectal projection; for localization of retinal axons to the retinorecipient laminae and for refinement of the retinotectal projection.

REFERENCES

Aihara, H. and Miyazaki, J. (1998). Gene transfer into muscle by electroporation in vivo. *Nat. Biotechnol.* **16**, 867-870.

Cavallo, R. A., Cox, R. T., Moline, M. M., Roose, J., Polevoy, G. A., Clevers, H., Peifer, M. and Bejsovec, A. (1998). Drosophila Tcf and Groucho interact to repress Wingless signalling activity. *Nature* **395**, 604-608.

Cepko, C. L., Ryder, E., Austin, C., Golden, J., Fields-Berry, S. and Lin, J. (2000). Lineage analysis with retroviral vectors. *Methods Enzymol.* **327**, 118-145.

Chen, G. and Courey, A. J. (2000). Groucho/TLE family proteins and transcriptional repression. *Gene* **249**, 1-16.

Cline, H. T., Debski, E. A. and Constantine-Paton, M. (1987). N-methyl-D-aspartate receptor antagonist desegregates eye-specific stripes. *Proc. Natl. Acad. Sci. USA* **84**, 4342-4345.

Courey, A. J. and Jia, S. (2001). Transcriptional repression: the long and the short of it. *Genes Dev.* **15**, 2786-2796.

Crossland, W. J., Cowan, W. M., Rogers, L. A. and Kelly, J. P. (1974). The specification of the retino-tectal projection in the chick. *J. Comp. Neurol.* **155**, 127-164.

Fagiolini, M. and Hensch, T. K. (2000). Inhibitory threshold for critical-period activation in primary visual cortex. *Nature* **404**, 183-186.

Fisher, A. L. and Caudy, M. (1998). Groucho proteins: transcriptional corepressors for specific subsets of DNA-binding transcription factors in vertebrates and invertebrates. *Genes Dev.* **12**, 1931-1940.

Fisher, A. L., Ohsako, S. and Caudy, M. (1996). The WRPW motif of the hairy-related basic helix-loop-helix repressor proteins acts as a 4-amino-acid transcription repression and protein-protein interaction domain. *Mol. Cell. Biol.* **16**, 2670-2677.

Funahashi, J., Okafuji, T., Ohuchi, H., Noji, S., Tanaka, H. and Nakamura, H. (1999). Role of Pax-5 in the regulation of a mid-hindbrain organizer's activity. *Dev. Growth Differ.* **41**, 59-72.

Gardner, C. A., Darnell, D. K., Poole, S. J., Ordahl, C. P. and Barald, K. F. (1988). Expression of an engrailed-like gene during development of the early embryonic chick nervous system. *J. Neurosci. Res.* **21**, 426-437.

Gray, G. E., Glover, J. C., Majors, J. and Sanes, J. R. (1988). Radial arrangement of clonally related cells in the chicken optic tectum: lineage analysis with a recombinant retrovirus. *Proc. Natl. Acad. Sci. USA* **85**, 7356-7360.

Gray, G. E. and Sanes, J. R. (1991). Migratory paths and phenotypic choices of clonally related cells in the avian optic tectum. *Neuron* **6**, 211-225.

Halliday, A. L. and Cepko, C. L. (1992). Generation and migration of cells in the developing striatum. *Neuron* **9**, 15-26.

Hamburger, V. and Hamilton, H. L. (1951). A series of normal stages in the development of the chick embryo. *J. Morphol.* **88**, 49-92.

Heasman, J., Kofron, M. and Wylie, C. (2000). Beta-catenin signaling activity dissected in the early Xenopus embryo: a novel antisense approach. *Dev. Biol.* **222**, 124-134.

Hevner, R. F., Shi, L., Justice, N., Hsueh, Y., Sheng, M., Smiga, S., Bulfone, A., Goffinet, A. M., Campagnoni, A. T. and Rubenstein, J. L. (2001). Tbr1 regulates differentiation of the preplate and layer 6. *Neuron* **29**, 353-366.

Hughes, S. H., Greenhouse, J. J., Petropoulos, C. J. and Sutrave, P. (1987). Adaptor plasmids simplify the insertion of foreign DNA into helper-independent retroviral vectors. *J. Virol.* **61**, 3004-3012.

Ishii, Y., Fukuda, K., Saiga, H., Matsushita, S. and Yasugi, S. (1997). Early specification of intestinal epithelium in the chicken embryo: a study on the localization and regulation of CdxA expression. *Dev. Growth Differ.* **39**, 643-653.

Jackson, C. A., Peduzzi, J. D. and Hickey, T. L. (1989). Visual cortex development in the ferret. I. Genesis and migration of visual cortical neurons. *J. Neurosci.* **9**, 1242-1253.

Jacobson, M. (1991). *Developmental Neurobiology*. New York: Plenum Press.

Jasoni, C. L., Walker, M. B., Morris, M. D. and Reh, T. A. (1994). A chicken achaete-scute homolog (CASH-1) is expressed in a temporally and spatially discrete manner in the developing nervous system. *Development* **120**, 769-783.

Jessell, T. M. (2000). Neuronal specification in the spinal cord: inductive signals and transcriptional codes. *Nat. Rev. Genet.* **1**, 20-29.

Kageyama, R. and Nakanishi, S. (1997). Helix-loop-helix factors in growth and differentiation of the vertebrate nervous system. *Curr. Opin. Genet.* **7**, 659-665.

Kishimoto, K. N., Watanabe, Y., Nakamura, H. and Kokubun, S. (2002) Ectopic bone formation by electroporatic transfer of bone morphogenetic protein-4 gene. *Bone* **31**, 340-347.

Kobayashi, T., Nakamura, H. and Yasuda, M. (1990). Disturbance of refinement of retinotectal projection in chick embryos by tetrodotoxin and grayanotoxin. *Dev. Brain Res.* **57**, 29-35.

Kröger, S. and Schwarz, U. (1990). The avian tectobulbar tract: development, explant culture, and effects of antibodies on the pattern of neurite outgrowth. *J. Neurosci*. **10**, 3118-3134.

LaVail, J. H. and Gowan, W. M. (1971a). The development of the chick optic tectum. I. Normal morphology and cytoarchitectonic development. *Brain Res.* **28**, 391-419.

LaVail, J. H. and Cowan, W. M. (1971b). The development of the chick optic tectum. II. Autoradiographic studies. *Brain Res.* **28**, 421-441.

Logan, C., Wizenmann, A., Drescher, U., Monschau, B., Bonhoeffer, F. and Lumsden, A. (1996). Rostral optic tectum acquires caudal characteristics following ectopic engrailed expression. *Curr. Biol.* **6**, 1006-1014.

Matsunaga, E., Araki, I. and Nakamura, H. (2000). Pax6 defines the di-mesencephalic boundary by repressing En1 and Pax2. *Development* **127**, 2357-2365.

McConnell, S. K. (1988). Fates of visual cortical neurons in the ferret after isochronic and heterochronic transplantation. *J. Neurosci.* **8**, 945-974.

McLoon, S. C. (1985). Evidence for shifting connections during development of the chick retinotectal projection. *J. Neurosci.* **5**, 2570-2580.

Meister, M., Wong, R. O., Baylor, D. A. and Shatz, C. J. (1991). Synchronous bursts of action potentials in ganglion cells of the developing mammalian retina. *Science* **252**, 939-943.

Mizuguchi, R., Sugimori, M., Takebayashi, H., Kosako, H., Nagao, M., Yoshida, S., Nabeshima, Y., Shimamura, K. and Nakafuku, M. (2001). Combinatorial roles of olig2 and neurogenin2 in the coordinated induction of pan-neuronal and subtype-specific properties of motoneurons. *Neuron* **13**, 757-771.

Momose, T., Tonegawa, A., Takeuchi, J., Ogawa, H., Umesono, K. and Yasuda, K. (1999). Efficient targeting of gene expression in chick embryos by microelectroporation. *Dev. Growth Differ*. **41**, 335-344.

Mooney, R., Penn, A. A., Gallego, R. and Shatz, C. J. (1996). Thalamic relay of spontaneous retinal activity prior to vision. *Neuron* **17**, 863-874.

Muhr, J., Andersson, E., Persson, M., Jessell, T. M. and Ericson, J. (2001). Groucho-mediated transcriptional repression establishes progenitor cell pattern and neuronal fate in the ventral neural tube. *Cell* **104**, 861-873.

Nakamura, H. and O'Leary, D. D. (1989). Inaccuracies in initial growth and arborization of chick retinotectal axons followed by course corrections and axon remodeling to develop topographic order. *J. Neurosci.* **9**, 3776-3795.

Nakamura, H., Watanabe, Y. and Funahashi, J. (2000). Misexpression of genes in brain vesicles by in ovo electroporation. *Dev. Growth Differ*. **42**, 199-201.

Novitch, B. G., Chen, A. I. and Jessell, T. M. (2001). Coordinate regulation of motor neuron subtype identity and pan-neuronal properties by the bHLH repressor Olig2. *Neuron* **13**, 773-789.

O'Leary, D. D., Fawcett, J. W. and Cowan, W. M. (1986). Topographic targeting errors in the retinocollicular projection and their elimination by selective ganglion cell death. *J. Neurosci.* **6**, 3692-3705.

Paroush, Z., Finley, R. L., Jr., Kidd, T., Wainwright, S. M., Ingham, P. W., Brent, R. and Ish-Horowicz, D. (1994). Groucho is required for Drosophila neurogenesis, segmentation, and sex determination and interacts directly with hairy-related bHLH proteins. *Cell* **79**, 805-815.

Pearlman, A. L., Faust, P. L., Hatten, M. E. and Brunstrom, J. E. (1998). New directions for neuronal migration. *Curr. Opin. Neurobiol*. **8**, 45-54.

Pierani, A., Moran-Rivard, L., Sunshine, M. J., Littman, D. R., Goulding, M. and Jessell, T. M. (2001). Control of interneuron fate in the developing spinal cord by the progenitor homeodomain protein Dbx1. *Neuron* **29**, 367-384.

Rager, G. and von Oeynhausen, B. (1979). Ingrowth and ramification of retinal fibers in the developing optic tectum of the chick embryo. *Exp. Brain Res*. **35**, 213-227.

Rice, D. S. and Curran, T. (1999). Mutant mice with scrambled brains: understanding the signaling pathways that control cell positioning in the CNS. *Genes Dev*. **13**, 2758-2773.

Roose, J., Molenaar, M., Peterson, J., Hurenkamp, J., Brantjes, H., Moerer, P., van de Wetering, M., Destree, O., and Clevers, H. (1998). The Xenopus Wnt effector XTcf-3 interacts with Groucho-related transcriptional repressors. *Nature* **395**, 608-612.

Shigetani, Y., Funahashi, J. I. and Nakamura, H. (1997). En-2 regulates the expression of the ligands for Eph type tyrosine kinases in chick embryonic tectum. *Neurosci. Res*. **27**, 211-217.

Stryker, M. P. and Harris, W. A. (1986). Binocular impulse blockade prevents the formation of ocular dominance columns in cat visual cortex. *J. Neurosci.* **6**, 2117-2133.

Suemori, H., Kadodawa, Y., Goto, K., Araki, I., Kondoh, H. and Nakatsuji, N. (1990). A mouse embryonic stem cell line showing pluripotency of differentiation in early embryos and ubiquitous beta-galactosidase expression. *Cell Differ. Dev*. **29**, 181-186.

Sugiyama, S., Funahashi, J. and Nakamura, H. (2000). Antagonizing activity of chick *Grg4* against tectum-organizing activity. *Dev. Biol.* **221**, 168-180.

Summerton, J. (1999). Morpholino antisense oligomers: the case for an RNase H-independent structural type. *Biochim. Biophys. Acta* **1489**, 141-158.

Thanos, S. and Bonhoeffer, F. (1987). Axonal arborization in the developing chick retinotectal system. *J. Comp. Neurol.* **261**, 155-164.

Uchikawa, M., Kamachi, Y. and Kondoh, H. (1999). Two distinct subgroups of Group B Sox genes for transcriptional activators and repressors: their expression during embryonic organogenesis of the chicken. *Mech. Dev*. **84**, 103-120.

Vallstedt, A., Muhr, J., Pattyn, A., Pierani, A., Mendelsohn, M., Sander, M., Jessell, T. M. and Ericson, J. (2001). Different levels of repressor activity assign redundant and specific roles to Nkx6 genes in motor neuron and interneuron specification. *Neuron* **13**, 743-755.

Wakamatsu, Y. and Weston, J. A. (1997). Sequential expression and role of Hu RNA-binding proteins during neurogenesis. *Development* **124**, 3449-3460.

Yamagata, M. and Sanes, J. R. (1995). Lamina-specific cues guide outgrowth and arborization of retinal axons in the optic tectum. *Development* **121**, 189-200.

Yamagata, M., Herman, J. P. and Sanes, J. R. (1995). Lamina-specific expression of adhesion molecules in developing chick optic tectum. *J. Neurosci*. **15**, 4556-4571.

Yao, J., Liu, Y., Lo, R., Tretjakoff, I., Peterson, A. and Stifani, S. (2000). Disrupted development of the cerebral hemispheres in transgenic mice expressing the mammalian Groucho homologue transducin-like-enhancer of split 1 in postmitotic neurons. *Mech. Dev*. **93**, 105-115.

Ye, W., Bouchard, M., Stone, D., Liu, X., Vella, F., Lee, J., Nakamura, H., Ang, S. L., Busslinger, M. and Rosenthal, A. (2001). Distinct regulators control the expression of the mid-hindbrain organizer signal, FGF8. *Nat. Neurosci*. **4**, 1175-1181.